

GODDARD SPACE FLIGHT CENTER

Evaluation Report

"The information contained herein is presented for guidance of employees of the Goddard Space Flight Center. It may be altered, revised, or rescinded due to subsequent developments or additional test results. These changes could be communicated internally by other Goddard publications. Notice is hereby given that this document is distributed outside of Goddard as a courtesy only to other government agencies and contractors and is understood to be only advisory in nature. Neither the United States Government nor any person acting on behalf of the United States Government assumes any liability resulting from the use of the information contained herein."

Microcircuit (24)
Mfr.: Hitachi
P/N: 58V1001T25
D/C: 9538

Project
PEM
System

Malfunction Report

Incoming Inspected

Requester
J. Kadesch (300.1)

Initiated Date
08/15/97

Purchase Specifications
commercial

Screening Specifications
commercial

Investigator
A.Teverovsky (300.1)

Technical Approval/Date

Approval for Distribution/Date

Background

Twenty four Hitachi 58V1001T25 microcircuits (SNs from 21 through 40, 46, 135, 136, and 137) were submitted to the GSFC Parts Analysis Laboratory for external visual and radiographic examinations and for an evaluation of their design.

Part Description

The Hitachi 58V1001T25 is an electrically erasable and programmable read-only memory (EEPROM) organized as 131072-word \times 8-bit (1 Mb). It has high speed and low power consumption by employing advanced MNOS memory technology and CMOS circuitry processing. The part is encapsulated in a 32-terminal thin, small-outline, plastic package (TSOP).

Analysis

1. External Examinations

All samples were subjected to external microscopic examinations (e.g. see Figure 1). No package warping, cracks, voids, or foreign inclusions in the plastic encapsulant were found. Practically all parts had gaps between the lead frame support bar and the molding compound on the side of the package (see Figure 2). Cross sectional examinations showed that these gaps were shallow and did not extend into packages more than 150-250 μ . Radiographic examination showed adequate wire bond dressing. Typical top and side X-ray views are shown in Figure 3. The die-paddle had holes which were probably designed to reduce voiding in die attach material, to enhance adhesion between the molding compound and lead frame, and to provide stress relief for the large die.

2. Internal Examinations

Four samples (SNs 38, 39, 40, and 41) were decapsulated in the red fuming nitric acid and examined microscopically. Figure 4 shows an overall view after decapsulation. Some bonding wires were exposed completely (both to die and lead frame). Bonds to the lead frame fingertips had evidence of acid attack from the decapsulation process. Aluminum discoloration was found at two contact pads in SN 40 (see Figure 5). No other defects were observed.

3. Bond-pull and ball-shear tests

Approximately half of the wires in samples SN 38 and SN 39 and all the wires in SN 40 were subjected to wire pull testing (a total of 56 wires). The test was performed per MIL-STD-883, TM 2011. Results are shown in Table 1. The wires which were exposed completely most often broke at the post bond (BC 3) and had much smaller pull forces compared to wires which broke at the neck (BC 1). Table 2 displays the statistics for two different break codes. The wires with BC 1 had an average pull force of 6.8 – 7.9 g-f and a coefficient of variance less than 20%. These values are typical for 1.2 mil gold wires. The average pull force for completely exposed wires was approximately 3-4 times less. The bonds to the lead frame weakening was most probably caused by decapsulation.

The rest (those not wire-pulled) of the wires in SN 38 and SN 39 and half of the wires in SN 40 were subjected to ball shear testing per ASTM F1269. Results of this test are shown in Tables 3. No failures (cratering, ball/bonding pad lift, or fracture along the intermetallic) occurred during this test. Distributions of the ball shear forces (see Figure 6) were distinctly bimodal. This was found to be due to the positioning of the shearing ram at the ball bond. Figure 7 shows views of two ball bonds which were sheared at a high and normal (approximately at the middle of the ball) positions of the shearing ram. Bonds which sheared at the top of the balls averaged 30 – 38 g-f (see Table 4) whereas bonds which sheared in the balls averaged at 66 – 81 g-f. A typical average shear force for 1 mil wires is 32 g-f with a coefficient of variance less than 25%. For wires of 1.2 mil diameter this value would be approximately 46 g-f. Although there is no official criteria for ball shear testing, ASTM F1269 regards a shear force of less than 15 g-f for 1 mil wires as rejectable. For 1.2 mil wires this limit would be 21 g-f. Table 3 shows that all properly sheared bonds (BC 2) had much larger shear forces. Several bonds which had been sheared with a high position of the ram (BC 1) had a “rejectable” force, but this most likely was caused by the test technique rather than indicating any bond problems.

Table 1. Wire pull test results.

Wire	SN 38		SN 39		SN 40		comments
	g - f	BC	g - f	BC	g - f	BC	

1			8.9	1	10.5	1	
2			5.1	3	8.8	1	
3			0.7	3	9.1	1	
4			4.2	3	6.3	1	
5			7.5	1	8.4	1	
6			5.5	1	8.6	1	
7			5.8	1	9.7	3	
8			7.3	1	6.9	1	
9			6.7	1	3.2	3	
10			4.4	2	1.2	3	
11			5	1	0.9	3	
12			6.8	1	0	3	
13			7.2	1	0	3	
14			8.6	1	3.6	3	
15					5.3	1	
16					0	1	broken during decapsulation
17					6.6	1	
18					7.4	1	
19					9.2	1	
20	4.6	1			8.2	1	
21					8.7	1	
22	8.4	2			1.5	3	Contact pad discoloration
23	6.5	1			0	3	Contact pad discoloration
24	7.4	1			2.8	3	Contact pad discoloration
25	6.1	1			1.1	3	Contact pad discoloration
26	6.5	1			4	3	
27	7.8	1			7.7	1	
28	7.7	1			7.8	1	
29	8	1			8.1	1	
30	5.6	2			6	1	
31					8.1	1	
32					8.4	2	

Break Code (BC): 1 – at the neck; 2 – in the span; 3 – at the post.

Table 2. Pull Test Statistics

Parameter	SN 38		SN 39		SN 40	
	BC 1	BC 3	BC 1	BC 3	BC 1	BC 3
QTY	8	0	10	3	19	12
Min	4.6	-	8.6	0.7	5.3	0
Max	8	-	8.9	5.1	10.5	9.7
Average	6.8	-	6.9	3.3	7.9	2.3
St. dev.	1.14	-	1.26	2.32	1.32	2.72

Table 3. Ball Shear Test Results.

Wire	SN 38		SN 39		SN 40	
	g - f	BC	g - f	BC	g - f	BC
1	23	1	38	1	80	2
2	33	1	65	2	28	1
3	33	1	68	2	33	1
4	35	1	45	1	35	1
5	25	1	38	1	38	1
6	80	2	48	1	20	1
7	108	2	55	2	20	1
8	38	1	33	1	23	1
9	40	1	33	1	28	1
10	88	2	40	1	33	1
11	88	2	78	2	38	1
12	80	2	28	1	68	2
13	85	2	38	1	38	1
14	73	2	43	1	38	1
15	80	2	38	1	93	2
16	88	2			23	1

Break Code (BC): 1 – at the top of the ball, 2 – at the middle of the ball

Table 4. Ball Shear Test Statistics

Parameter	SN 38		SN 39		SN 40	
	BC 1	BC 2	BC 1	BC 2	BC 1	BC 2
QTY	6	10	11	4	13	3
Min	23	40	28	55	20	68
Max	38	108	48	78	38	93
Average	31.2	81	38.4	66.5	30.4	80.3
St. dev.	5.88	17.13	5.71	9.47	7.09	12.50

4. Glassivation integrity

This examination was performed on two samples (SN 38 and SN 39) per MIL-STD-883D, Method 2021, "Glassivation layer integrity". This involved a high power optical examination after the die was subjected to an aluminum etch. No glassivation defects were observed.

5. SEM glassivation and bond examinations

Bonds and glassivation in sample SN 40 were inspected using a SEM. No glassivation defects were found. Energy-dispersive X-ray microanalysis (EDX) revealed that the glassivation was composed of a silicon oxide film covered with a nitride film.

Bond pad examination revealed that the contact pads which appeared discolored actually had no aluminum around the ball bonds. Figures 8 and 9 give SEM views and X-ray mapping of a "normal" contact pad (Figure 8) and a contact pad with apparent discoloration (Figure 9). Metallization at these pads was attacked by chemicals during deprocessing (decapsulation in red fuming nitric acid and rinsing in acetone and isopropanol). As all these chemicals do not normally react with aluminum, the reason for the etching at some of the contact pads is not clear.

6. SEM inspection of metallization

The metallization was inspected in SNs 38 and 39 per MIL-STD-883D, Method 2018 after glassivation removal. No rejectable defects were found. The planarization technique used in the microcircuit design eliminated possible step coverage problems. Figure 10 gives a view of the metallization. EDX analysis showed that molybdenum (approximately 0.1 μ) was used as a metallization barrier layer. Metal notches (mousebites) in the aluminum metallization were observed. These were probably due to galvanic corrosion of Si-Al precipitates during glassivation etching and/or rinsing and most likely are artifacts caused by deprocessing.

7. Cross Sectional Examinations

Two samples (SN 34 and SN 35) were cross sectioned at six planes and were examined using a high power optical microscope and a SEM.

7.1. Molding compound and lead frame.

The molding compound was filled with a mixture of a spherical and ground fused silica. Bromine was detected in the EDX spectrum of the molding compound indicating a brominated epoxy resin. Particles of several micrometers in size were found embedded into the polymer matrix. EDX analysis revealed antimony (Sb) and oxygen (O) in their composition indicating most likely antimony trioxide, which is used as a flame retardant. The molding compound had no cracks or big voids and formed intimate contact to all internal surfaces (die, wires, and lead frame). No gaps and/or delaminations were observed along the molding compound-lead frame interfaces (see Figures 11 and 12). Iron (Fe) and nickel (Ni) were detected in the lead frame composition indicating an Alloy-42 lead frame. External parts of the lead frame were tinned.

7.2. Die-to-molding compound interface.

The die was coated above the glassivation with a conformal coating (probably polyimide) approximately 2 μ thick (see Figure 13). No delaminations or gaps between the glassivation and the coating or between the coating and the molding compound were observed.

7.3. Wire-to-lead frame bonds.

The inner lead tips were spot-plated with silver (approximately 3-4 μ thick). Figures 14 and 15 are views of the wire-to-lead frame cross section. Gold wires formed adequate metallurgical contacts with silver plating at all examined wire-to-lead frame bonds.

7.4. Wire-to-die pad bonds.

Figure 16 gives an optical view and Figures 17 and 18 give SEM views of typical ball bond cross sections. Aluminum metallization under the contact pads was mostly consumed to form an Au/Al intermetallic layer 2 - 4 μ thick. Voids observed in the aluminum metallization around the contact pads probably were artifacts caused by corrosion during cross sectioning.

7.5. Die attachment.

The die was mounted to the lead frame base with a silver epoxy (probably to provide better die-to-paddle thermal conductivity than nonconductive epoxies). The thickness of the silver epoxy layer was approximately 5 μ . The silver filler was nonuniformly distributed along the adhesive layer (see Figure 19). No delaminations or excessive voiding at the die attachment were found. The silver epoxy adhesive did not spread properly near the die edges where the gaps were filled with molding compound (see Figure 11). These defects indicate some problems with the manufacturer's control over the die attachment process, but most likely would not seriously affect performance or reliability of the part.

Discussion

Au/Al intermetallic growth in the gold wire - aluminum contact pad bonds has historically been a major concern for the wire bond integrity. Intermetallic compounds are hard and brittle, but usually strong and conductive, and in itself do not normally degrade the performance of the bonds. However, the difference in diffusion flows of Al and Au may result in void (Kirkendall void) formation near the intermetallic region (mostly in Al rich side). This weakens the bond, increases its resistance, and may result in failure.

It is generally accepted that, if a die is wirebonded using a thermosonic process at less than 200 °C and is stored or operated at less than 150 °C, then the Au/Al system provides a reliable bond. However, even at relatively low temperatures, intermetallic formation continues to some degree. Experiments have showed that after approximately 1000 hr of operational life (at 145°C) the Au/Al intermetallic grew from 1.2-1.6 μ to 11-12 μ and most of the Al under the Au ball has been consumed.

The use of plastic packages and thin (1 μ or less) aluminum films at contact pads in contemporary IC chips also raises concern about Au/Al bond reliability due to a possible "dry corrosion" process and Kirkendall void formation along the periphery of the bonds.

A post-mold bake at +175 °C for 5 hours (minimum) usually is required to cure the molding compound. Calculation indicates that approximately 13 hours at this temperature will convert a 1 μ aluminum film to an intermetallic compound. Thus bond pads with thin aluminum contact pads are at least partially converted to Au₂Al, leaving the underlying structure highly stressed. Once the Al has been consumed under the ball bond, Kirkendall voiding under the bond and/or around its periphery will begin to occur. Even if the bond is still mechanically strong, it can have a high electrical resistance or open circuit due to the voids which have been formed around the bond periphery.

Another cause of Au/Al ball bond failures in epoxy encapsulated devices, “dry corrosion”, results due to Br ion release from brominated epoxy resin used in molding compound formulation as a flame retardant. The newest epoxy encapsulants have little free Br- and appear to cause negligible bond degradation unless the epoxy is degraded by high temperature (approximately 250 °C). The presence of antimony trioxide (Sb₂O₃) also can lead to rapid failures. Experiments with different molding compounds have been performed to estimate the Sb₂O₃ effect on Au/Al bond reliability. The median ball shear time-to-failure (τ_{50}) during aging at 200 °C was more than 2200 hours for compounds without Sb₂O₃ and less than 100 hours for compound with Sb₂O₃. High temperature and high humidity aging at 158 °C/85% gave τ_{50} =550 hours for the first compound and τ_{50} <100 hours for the second. It is believed that ball bond degradation can still be a serious problem under more mild and commonly found conditions. Moisture increases degradation of the bonds most likely by increasing the transport of corrosive ions (e.g. Br-, Sb+) to the ball/intermetallic interface. Ball shear which initially occurred through the gold ball changed to fracture in the interface between the gold ball and intermetallic region.

In our case both types of flame retardants (brominated epoxy and antimony trioxide filler) were used. The purpose of this is not clear, but both components may cause Au/Al bond degradation. In combination with thin aluminum contact pads this may create a serious reliability problem, especially if the parts are intended to be used under harsh (high temperature, and/or moisture, and/or thermal cycling) conditions.

Conclusions

An evaluation of the Hitachi 58V1001T25 EEPROM encapsulated in a plastic package revealed adequate integrity of the part. The molding compound had intimate contact with the die (covered with conformal coating), wires, and lead frame. The die was properly mounted to the lead frame base with a thin layer of silver epoxy. Both wire bonding (to contact pads and to lead frame) formed adequate metallurgical contacts. The thickness of the Au/Al intermetallic was 2-4 μ and the aluminum under the bond was mostly consumed. No rejectable defects were observed during glassivation integrity and SEM examinations.

Bromine (Br) and antimony (Sb) were detected in the molding compound X-ray spectrum. This indicates that brominated epoxy and antimony trioxide filler were used in the molding compound composition as flame retardants. Both components are known to deteriorate Au/Al bonds under high temperature and/or high humidity conditions. To ensure the quality of the parts, additional testing and evaluation, including aging at high temperature and/or humidity (possibly followed by multiple thermal cycles) are recommended.



Figure 1. An overall view of the Hitachi EEPROM. (7.5X)

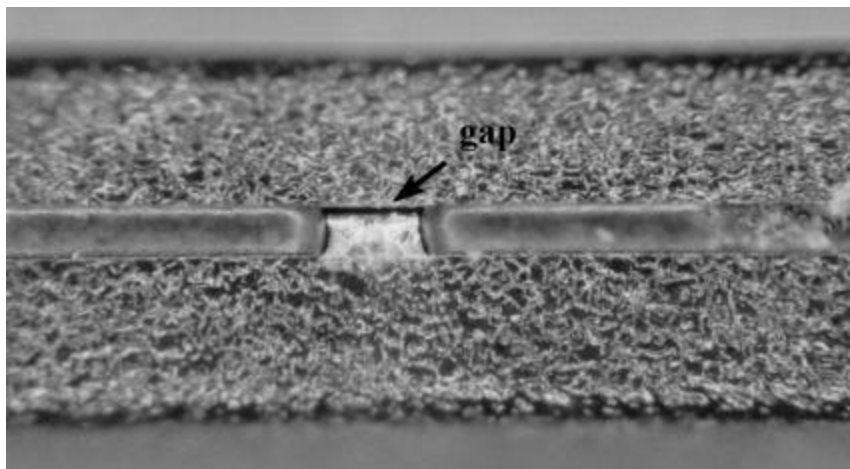


Figure 2. Side view of the package. (50X)

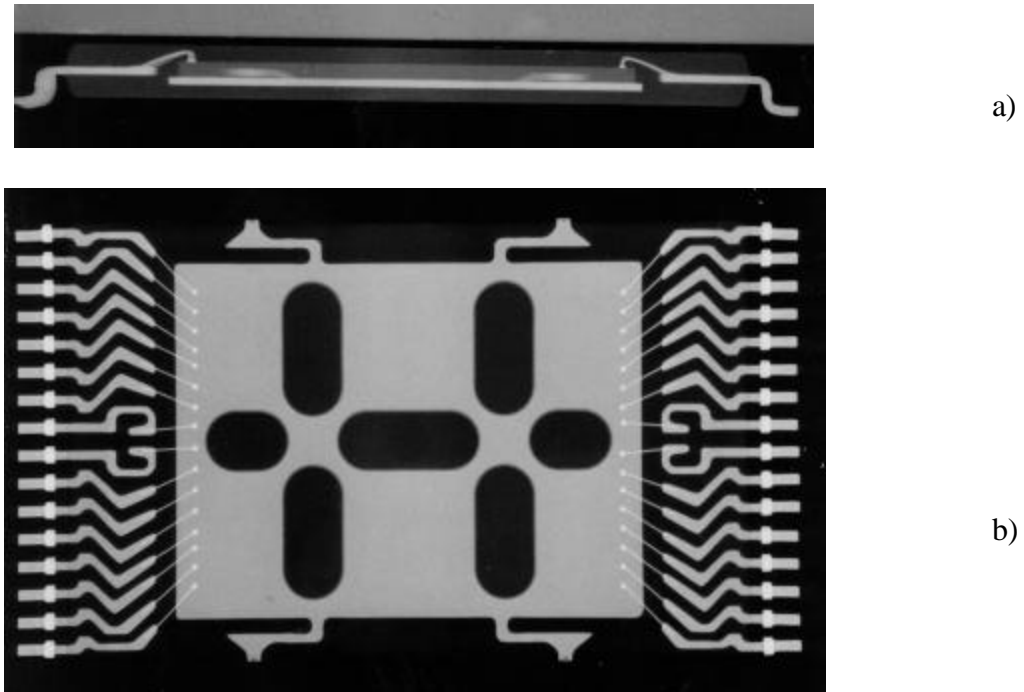


Figure 3. Side (a) and top (b) X-ray views of the microcircuit. (6X)

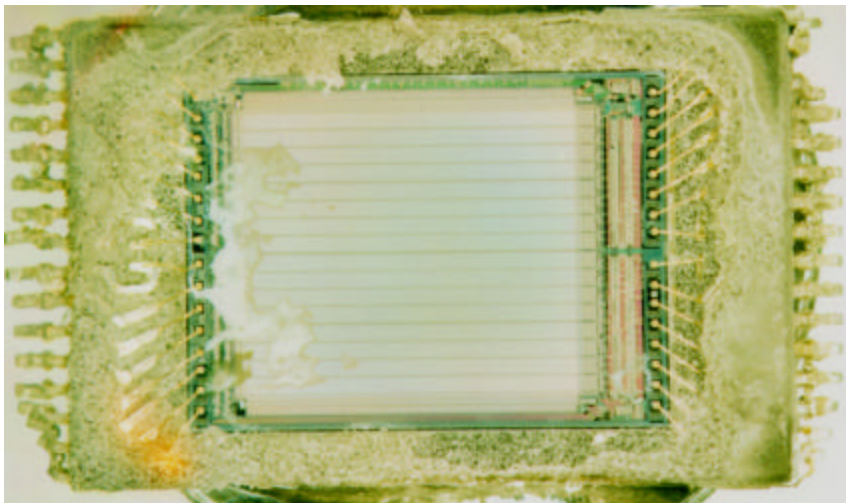


Figure 4. Overall view of the microcircuit after decapsulation, SN 39. (7.5X)

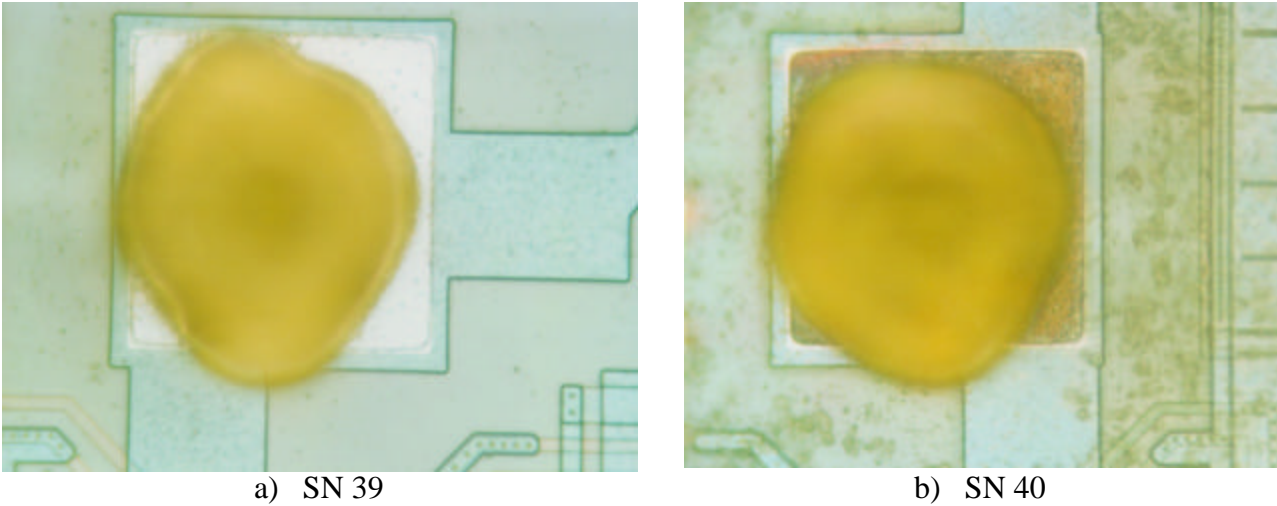


Figure 5. A normal contact pad (a) and a contact pad with aluminum discoloration. (500X)

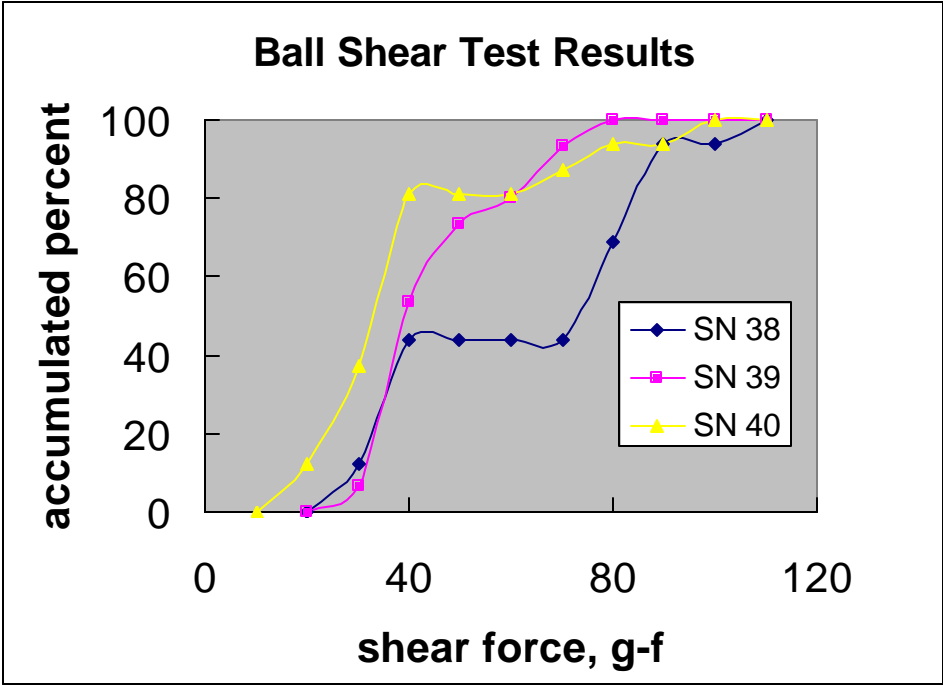
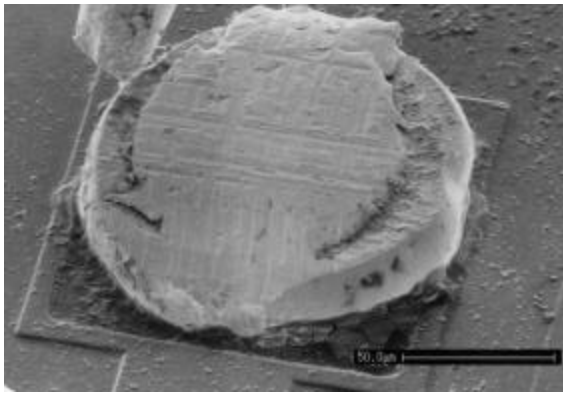
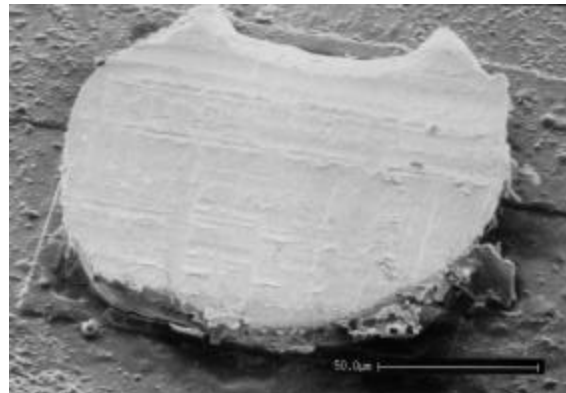


Figure 6. Shear force distributions.

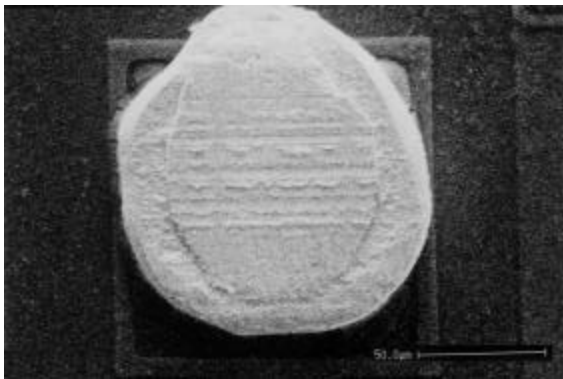


a) high position of the shearing ram

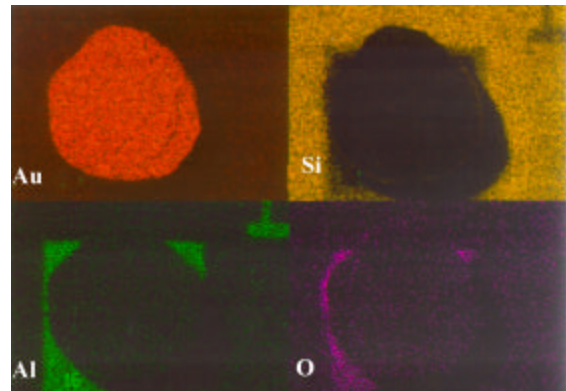


b) normal position of the shearing ram

Figure 7. SEM views of two bonds after ball shear test



a)



b)

Figure 8. SEM view (a) and X-ray mapping of a normal contact pad showing Al around the gold wire ball, SN 40.

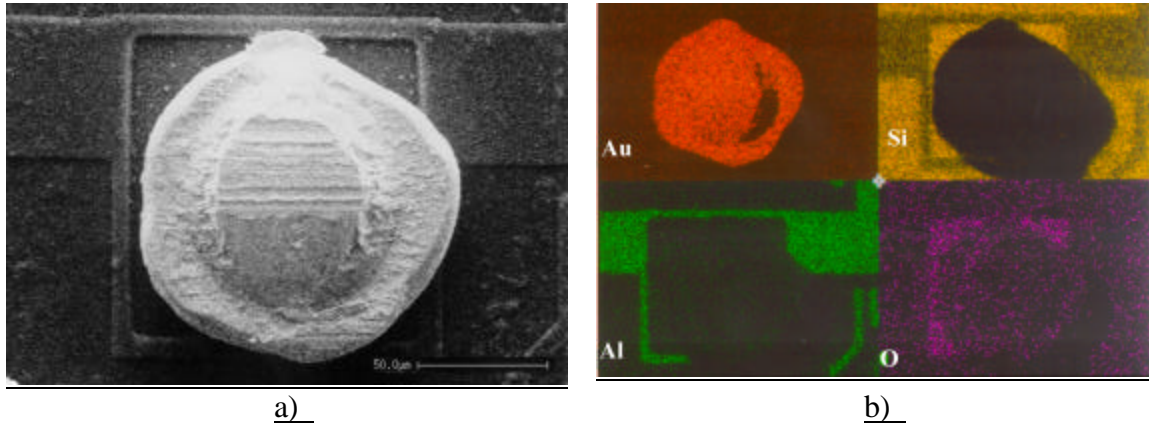


Figure 9. SEM view (a) and X-ray mapping of a “discolored” contact pad. No aluminum was detected around the gold wire ball, SN 40.

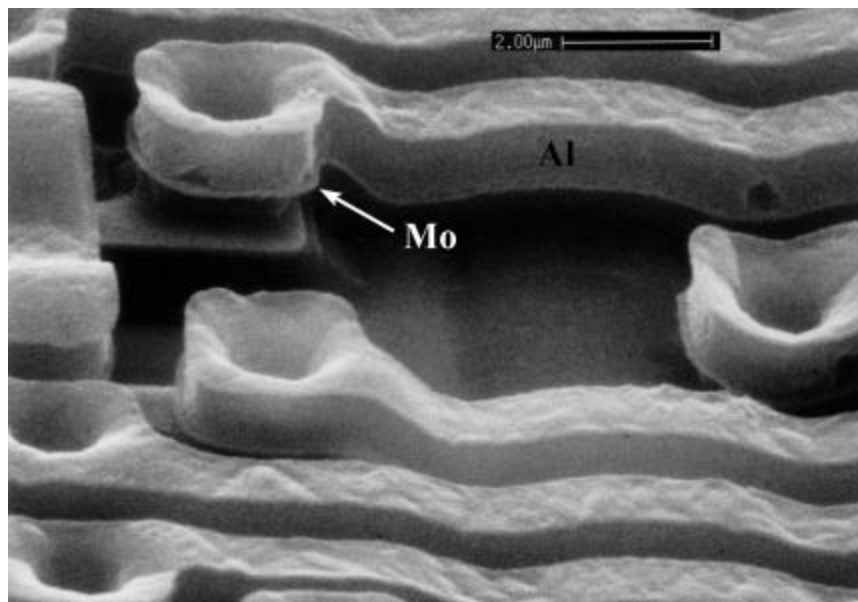


Figure 10. Typical SEM view of aluminum metallization, SN 39. (9890X)

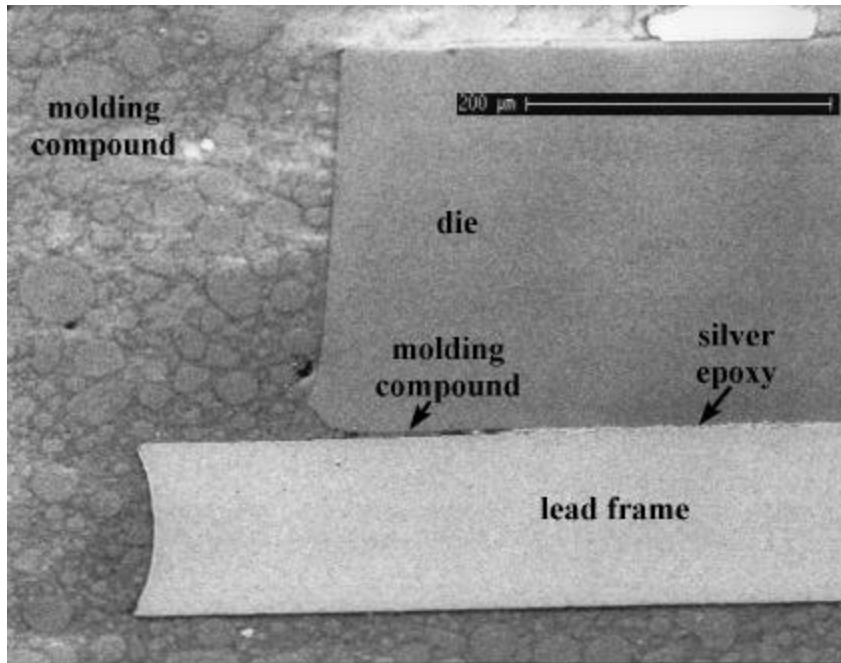


Figure 11. General SEM view of the cross section, SN 34, plane 6. (199X)

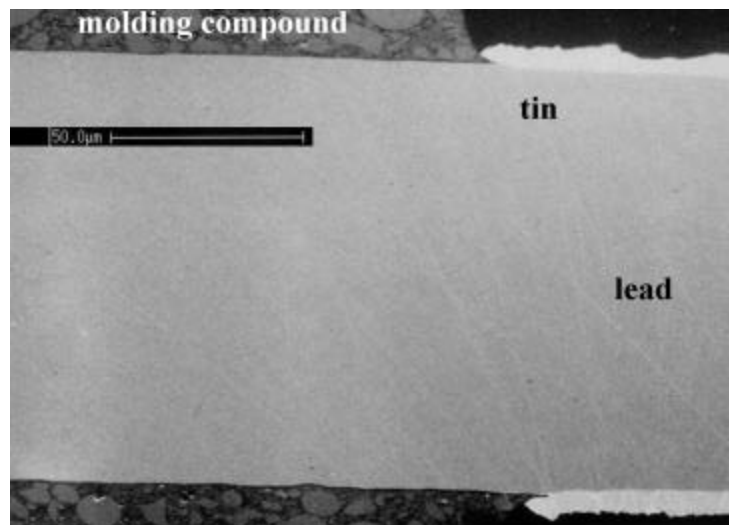


Figure 12. SEM view of the molding compound-to-lead frame cross section, SN 34, plane 4. (580X)

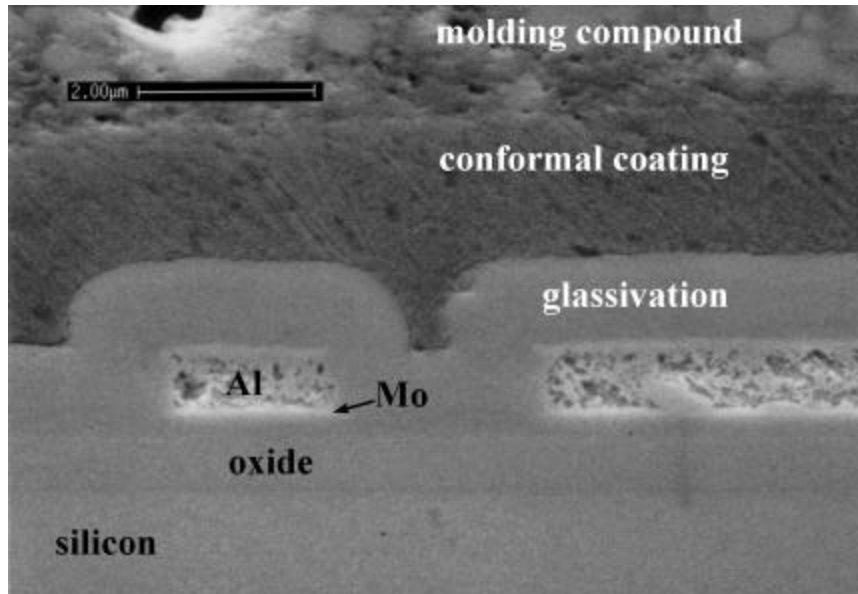


Figure 13. SEM view of the molding compound-to-die interface. (11,600X)

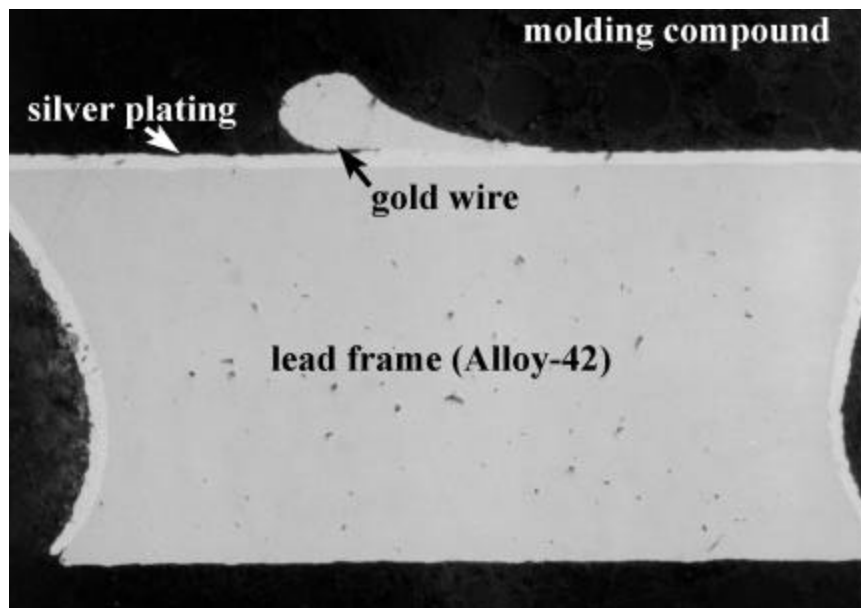


Figure 14. Optical view of the wire-to-lead frame cross section, SN 34, plane 4. (400X).

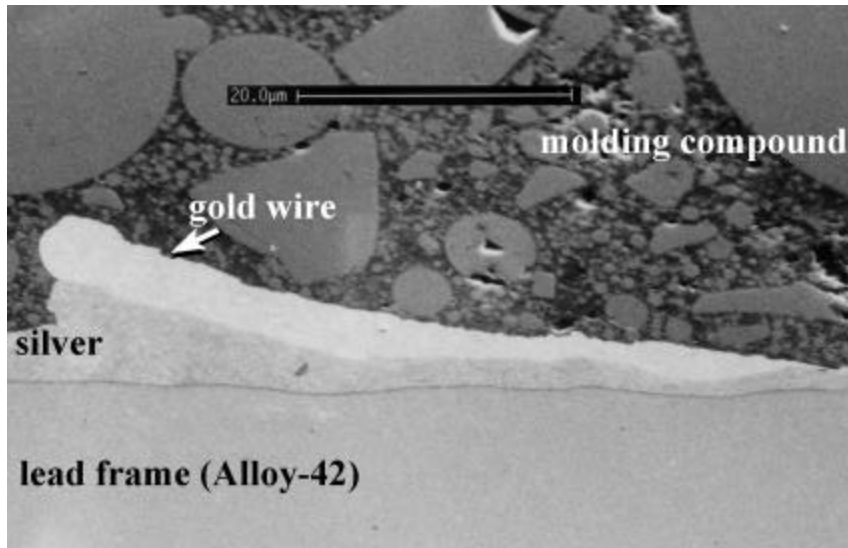


Figure 15. SEM view of the wire-to-lead frame cross section, SN 34, plane 4A. (1810X).

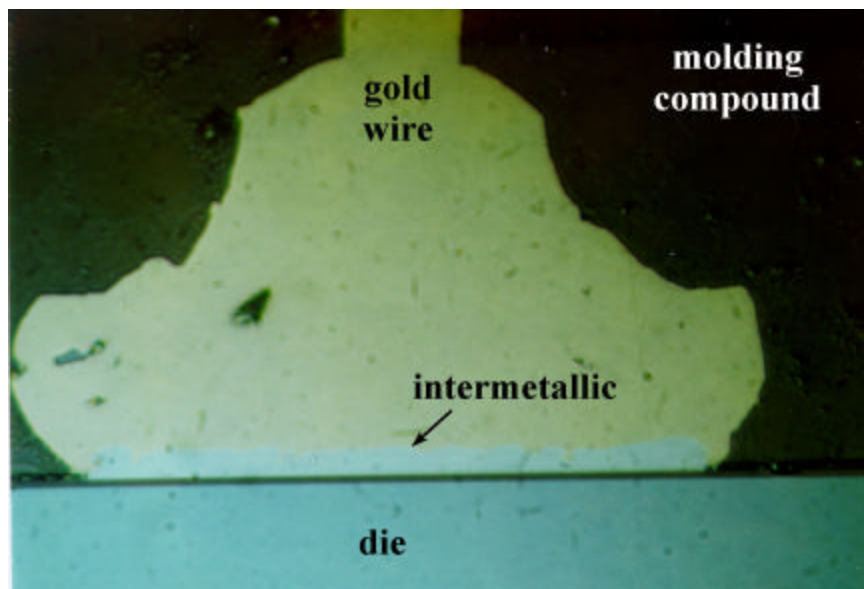


Figure 16. Optical view of the wire-to-contact pad cross section, SN 35, plane 3. (1000X).

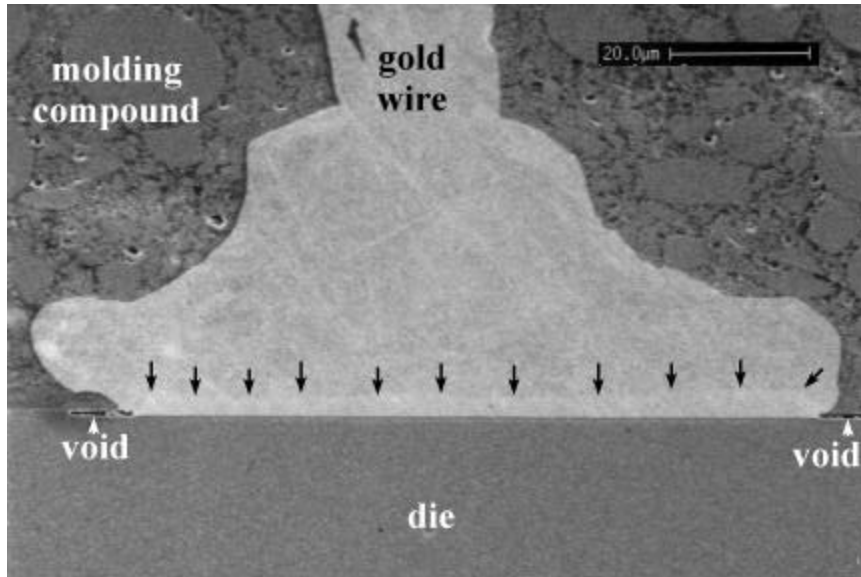


Figure 17. SEM view of the wire-to-contact pad cross section, SN 34, plane 6. (920X).

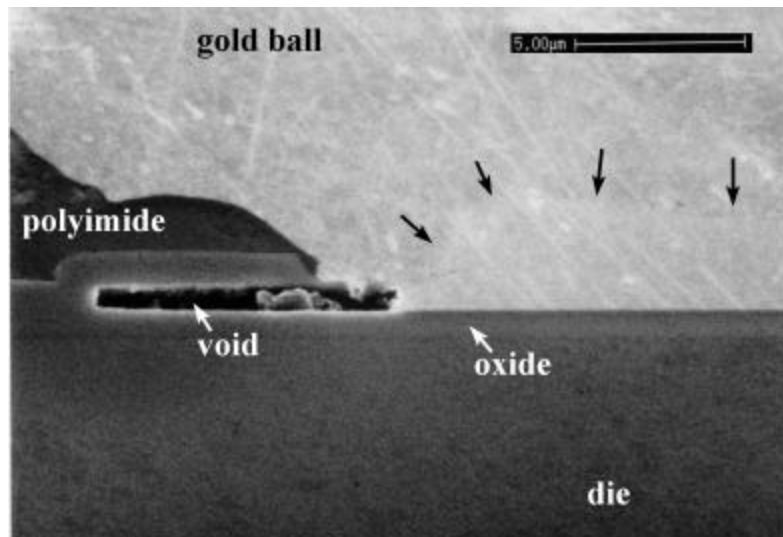


Figure 18. Close-up of the view shown above. (4900X)

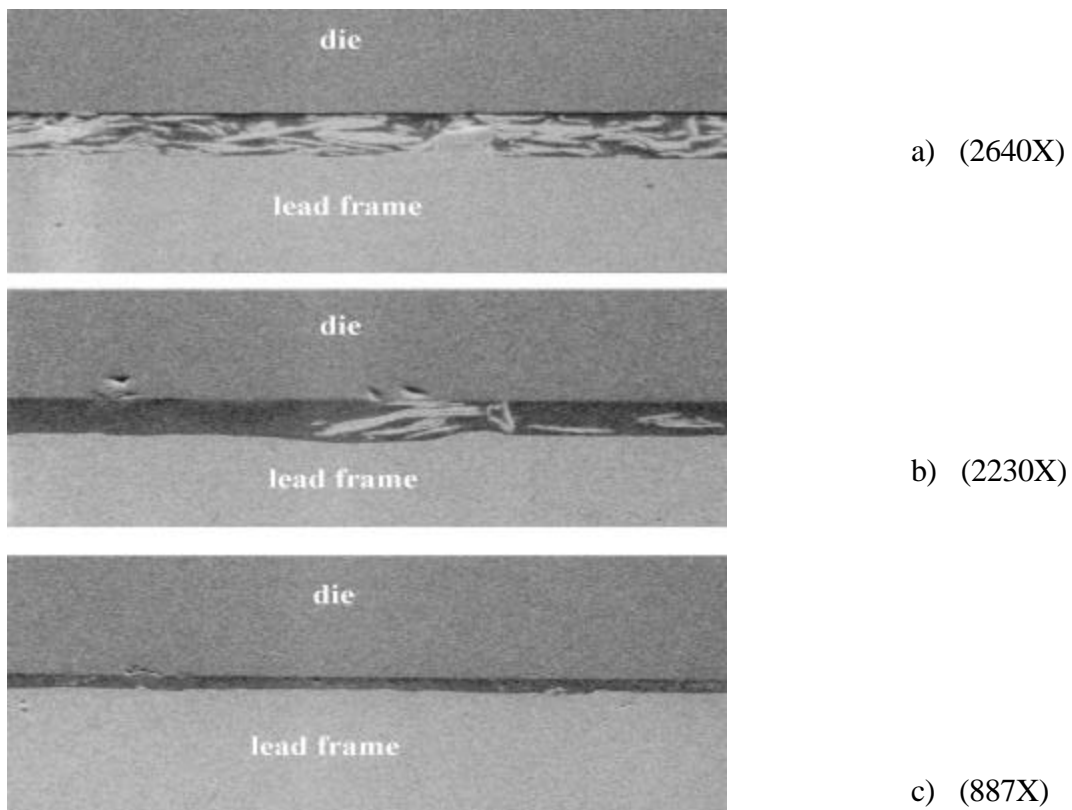


Figure 19. Three views of sections of the die attachment showing nonuniformity in silver distribution, SN 34, plane 4A.

“Intermetallic compound is hard and brittle, but strong and conductive, and in itself does not degrade the performance of the bond. The presence of voids under the bond, due to the Kirkendall effect, tends to weaken the bond strength and increase the resistance. The voids form due to differing rates of diffusion of Al and Au. Opens can occur in the Al some distance from the bond, due to mass transport of ions. It is generally accepted that if the device is stored or operated at $T < 150^{\circ}\text{C}$ then the Au/Al system provides a reliable bond.

Intermetal growth issue has historically been a major concern of the wire bond integrity. The vacancies coalesce to form Kirk voids.”

‘Al diffuses into Au rich compound (Au_5Al_2), leaving voids at the boundary (Kirk voids). T/S bonding reduces T to 200°C ’

Au/Al ball bond failure in epoxy encapsulated devices can occur due to “dry corrosion” resulting principally from the Br ion released from the encapsulant. The presence of antimony trioxide (Sb_2O_3) also leads to rapid failure. Ball shear initially occurred through the gold ball but changed to fracture in the interface between the gold ball and intermetallic region. Estimated median ball shear failure time

during aging at 200C was >2200 h for the compound without SB and less than 100 h for the comp with Sb. High temperature and high humidity aging at 158C/85% gave T50=550 h for the first compound and <100 h for the second. It is believed that the ball bond degradation can be a serious problem under more mild and commonly found conditions than was originally believed. The accelerating effect of moisture might result from increased transport of corrosive ions (e.g. Br-, Sb+) by moisture to the ball/intermetallic interface.

Intermetallic region of approximately 2.5 mkm in thickness was found with no visible signs of voiding

Once the Al has been consumed under the ball bond, K voiding will begin to occur.

Ball shear is more sensitive to intermetallic formation.

Failure mode associated with Au/Al intermetallic. The bond may be mechanically strong, but can have a high electrical resistance or may be even open-circuited. In this case, which typically occurs with gold wire bonded to thin (1mkm) Al metallization, voids form around the bond periphery limiting the available conductive path.

Bonds degrade by free halogen (Br-) ion. The newest epoxy encapsulants have little free Br- and appear to cause negligible bond degradation until the epoxy is degraded by high temp (approx 250C).

PEM require a post-mold bake of 5 h (min) at 175C, and a calculation indicates that approx 13 h will convert 1 mkm of Al to an intermetallic compound. Thus, most bond pads in PEM are at least partially converted to Au₂Al, leaving the underlying structure highly stressed.

Gold ball bonds (1 mil wire) sheared at an average of 60-80 g-f. Wire pull data indicated that gold wire pull strength averaged 8-10 g-f.

Intermetallic thickness for Au/Al bonding is more than 1 order of magnitude greater than for Cu/Al bonding. Experiments showed that after approximately 1000 hr of operation life (at 145°C), the Au/Al intermetallic grew from 1.2-1.6 μ to 11-12 μ. Most of the Al under the Au ball has been consumed while most of the Al remained under Cu ball bond.

A certain level of intermetallic formations is necessary to provide adequate bonding. In the case of Au/Al bonding, intermetallic layers can be observed during cross sectioning examinations. In this cross sectional and internal examination no intermetallic Cu/Al formations were detected. This is most likely due to the fact that the thickness of Cu/Al intermetallic layer did not exceed 0.1 μ.